Efficiency Degradation Caused by an Axial Feed Defocusing in Generalized Classical Axially-Symmetric Dual-Reflector Antennas

Fernando J. S. Moreira

Abstract— **The present work investigates the efficiency decay due to small axial feed displacements in classical axially-symmetric dual-reflector antennas. Analytical expressions for the antenna aperture field were previously derived from Geometrical Optics principles. These expressions enable the study of the aperture aberration dependence on small feed displacements and the consequent decrease in antenna efficiency. Parametric studies are conducted, in a generalized way, for the complete set of classical axially-symmetric dual-reflector antennas. Some representative geometries are further analyzed by the Moment Method to determine the accuracy of the present formulation.**

Index Terms— **Reflector antennas, aperture radiation, feed defocusing.**

I. Introduction

Dual-reflector antennas are widely used in high-gain applications such as satellite communications and radio astronomy. In axially-symmetric configurations, the aperture blockage offered by the subreflector and its supporting structure precludes the achievement of a uniform aperture-field distribution and, consequently, reduces the antenna efficiency. In some applications, the antenna performance is improved via reflector shaping. However, previous works have dealt with alternative classical axially-symmetric dual-reflector geometries yielding efficiencies higher than those typically obtained by the classical Cassegrain and Gregorian antennas [1]–[4]. These alternative reflector antennas are classified into four distinct configurations: Axially Displaced Cassegrain (ADC), Gregorian (ADG), Ellipse (ADE), and Hyperbola (ADH) [2]–[4]. The basic parameters of their classical generating curves (a parabola for the main reflector and an ellipse or a hyperbola for the subreflector) are depicted in Figs. 1–4, respectively. The three-dimensional surfaces are yielded by spinning the generating curves around the symmetry axis. Using Geometrical Optics (GO) principles, closed-form expressions were derived, in a generalized way, for their design, as well as for their aperture-field distribution [2],[3]. The formulation was further applied on a parametric study to determine their aperture efficiencies and, consequently, the optimum geometries [4]. In principle, efficiencies beyond 90% can be attained [4].

Manuscript received March 8, 1999.

Fernando J. S. Moreira, Federal University of Minas Gerais, Dept. Electronics Engineering, Av. Pres. Antonio Carlos 6627, Pampulha, Caixa Postal 209, 30161-970 Belo Horizonte, MG, Brazil, Tel. (+5531) 499-4861, FAX (+5531) 499-4850, fernando@eee.ufmg.br.

Five relevant input parameters are used to design the antennas: D_M, D_S, D_B (the main-reflector, subreflector, and blockage diameters, respectively), θ_E (the subreflector edge angle), and ℓ_o (the total ray-path from the primary focus to the aperture at the plane $z = 0$). Specific details about the antenna design are found in [2]. Nevertheless, when the tilt angle β (see Figs. 1–4) is null, the ADC and the ADG become the classical Cassegrain and Gregorian configurations, respectively. However, under the same circumstances ($\beta = 0$) both ADE and ADH are not feasible as the subreflector surface degenerate into a point (i.e., $D_S = 0$).

From the analytical expressions of the GO aperture field and the corresponding transformation of the input feed ray into the output aperture point, it is possible to investigate the aberrations caused by a small feed displacement from the antenna primary focus and the consequent decay of the radiation efficiency. The present work is concerned with the effects caused by a small axial feed defocusing. Such study is of great interest in the design of reflector antennas operating over a wide frequency range (as the feed phase center moves with the frequency) and in applications where the feed is axially displaced to achieve a broader main-beam pattern. In Sect. II, analytical expressions are derived for the aperture aberration as a function of the feed position over the symmetry axis. The adopted analysis is based on previous works conducted by Dragone, where the feed displacement is assumed small compared to the overall antenna geometry and to the radiation wavelength [5]. In Sect. III, the formulation is applied on a parametric investigation of the efficiency decrease with the feed location for several antenna geometries. As GO does not consider diffraction effects, in Sect. IV some representative antennas are numerically analyzed by the Moment-Method (MoM) technique and the results compared with those obtained by the present formulation to determine its accuracy and range of validity. The conclusions are presented in Sect. V.

II. The Aperture Aberration Function

The aberration function describes the phase distribution of the aperture field. Its derivation follows the procedure in [5], where a small feed displacement is considered. Let z_F be the z-coordinate of the feed location over the symmetry axis ($x_F = y_F = 0$), with $z_F = 0$ meaning that the spherical feed source is located at the antenna

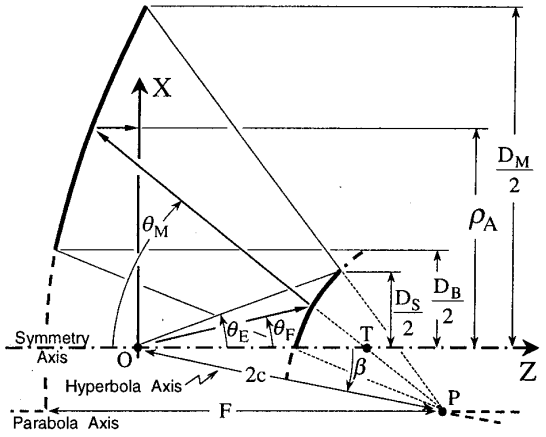

Fig. 1. ADC configuration.

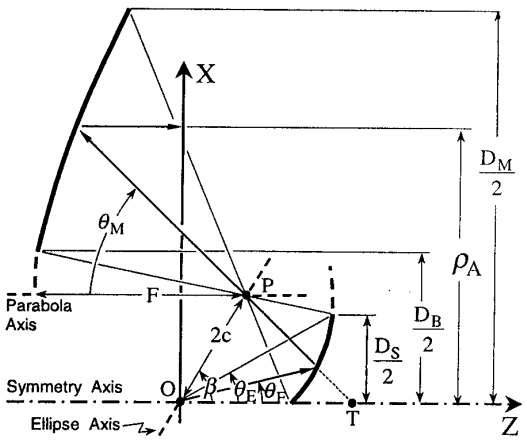

Fig. 3. ADE configuration.

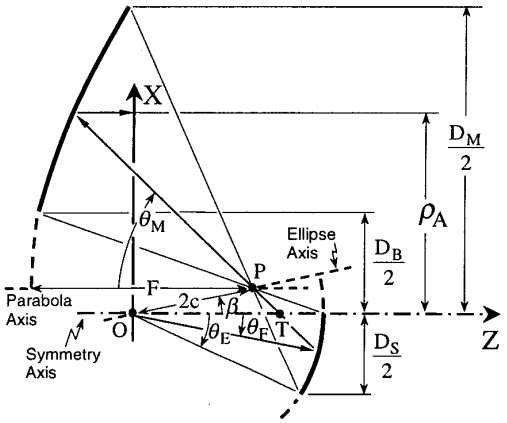

Fig. 2. ADG configuration.

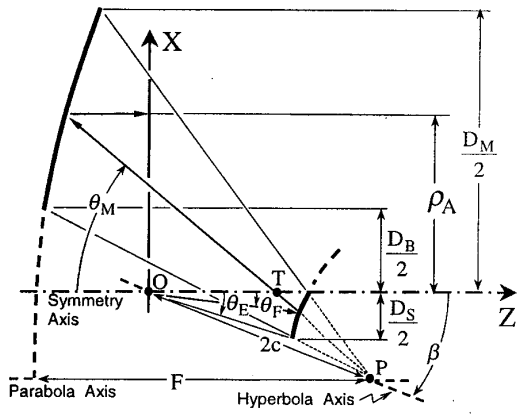

Fig. 4. ADH configuration.

primary focus (see Figs. 1–4). For small values of $|z_F|$ it can be shown that [5]

$$V(z_F,\theta_F) \approx \ell_o - z_F \cos\theta_F\,, \tag{1}$$

where $V(z_F,\theta_F)$ is the ray-path from the feed source to the corresponding aperture point (at the plane $z = 0$) and $\cos\theta_F$ is the direction cosine of the input feed ray (see Figs. 1–4). The second term at the right-hand side of (1) is the aberration function for the present case. Due to the circular symmetry, there is no azimuthal dependence.

At the aperture, it is convenient to express V as a function of ρ_A (the radial distance of the aperture point), whose dependence with θ_F is given by [2]:

$$\tan\left(\frac{\theta_F}{2}\right) = \frac{2\,A_3 - A_1\,\rho_A}{2\,A_4 - A_2\,\rho_A}\,, \tag{2}$$

where

$$A_1 = 1 - e\cos\beta\,, \tag{3}$$
$$A_2 = e\sin\beta\,, \tag{4}$$
$$A_3 = (c\,A_1 + e\,F)\sin\beta\,, \tag{5}$$
$$A_4 = F(1 + e\cos\beta) + c\,A_2\sin\beta\,, \tag{6}$$

F is the focal length of the main-reflector generating parabola, and e and $2c$ are the eccentricity and the inter-focal distance of the subreflector generating ellipse/hyperbola, respectively (see Figs. 1–4). Note that $0 < e < 1$ for the ADG and the ADE, while $|e| > 1$ for the ADC and the ADH [2],[3]. The problem at hand can be treated in a general way (i.e., for the four different configurations) by defining counterclockwise (clockwise) angles in the plane of Figs. 1–4 as positive (negative) an-

gles. From (2)–(6) one obtains

$$\cos\theta_F = \frac{(2A_4 - A_2\rho_A)^2 - (2A_3 - A_1\rho_A)^2}{(2A_4 - A_2\rho_A)^2 + (2A_3 - A_1\rho_A)^2}, \quad (7)$$

which can be expanded into powers of ρ_A yielding

$$\cos\theta_F = \sum_{i=0}^{\infty} B_i\,(\rho_A)^i. \quad (8)$$

The coefficients B_i can be written in terms of A_1, A_2, A_3, and A_4 with the help of [6]. The constant term B_0 in (8) does not affect the antenna efficiency. Furthermore, it can be shown that the coefficient B_1 is null whenever $\beta = 0$ or $e^2 = 1$. The former condition occurs for the classical Cassegrain and Gregorian antennas (obtained from the ADC and ADG, respectively, as previously discussed in Sect. I), where the defocus $(\rho_A)^2$ is already known to be the prominent aberration when the feed is axially displaced. The later condition is never met for practical antennas, as the subreflector generating curve tends to a parabola and, consequently, $2c \to \infty$. It can also be shown that as $|\beta| \to 0$ and $e^2 \to 1$ the aperture becomes less aberrated for a fixed value of z_F.

III. Parametric Study of the Aperture Efficiency Decrease

The basic antenna radiation characteristics (e.g., gain, efficiency, radiation pattern, etc.) can be calculated from the GO aperture field distribution. However, diffraction effects are ignored by GO and this might be a significant source of inaccuracy in all but reflector systems with very large electric dimensions (when GO is the dominant effect). Besides, the GO aperture field distribution also neglects the direct feed contribution to the antenna radiation pattern, multiple bounces over the reflector structure, etc.. In any event, for antenna-design purposes the information contained in the GO aperture distribution is very useful and, in this section, it will be adopted to study the aperture efficiency of the present antennas.

The previous formulation was employed on a parametric investigation of the aperture efficiency (η_A) decay with z_F. This was accomplished by integrating the GO aperture field to obtain the antenna far-zone radiation. Assuming that $|z_F|$ is sufficiently small, the change in the aperture-amplitude distribution does not significantly affect the antenna efficiency [5]. For this reason the amplitude distribution at the aperture was assumed unaltered and the associated phase determined from (1)–(8). Complete closed-form expressions for the GO aperture field when $z_F = 0$ are found in [2].

The antenna efficiency η_A accounts for the spillover loss (assuming $z_F = 0$) and the aperture illumination efficiency (with respect to a uniformly illuminated aperture with diameter D_M), such that the antenna boresight gain is given by [7]

$$G(\theta = 0°) = \eta_A \left(\frac{\pi D_M}{\lambda}\right)^2, \quad (9)$$

where λ is the radiation wavelength. Due to the adopted GO principles, similar antennas (antennas with identical angular dimensions) will have the same efficiency η_A provided that the same feed illumination and the same z_F/λ are adopted. For this reason the parametric investigation was conducted with the antenna linear dimensions normalized to D_M and with z_F expressed in terms of λ. The values of $D_S = D_B = 0.1\,D_M$ were chosen aiming highly efficient antennas, based on previous results in [4]. The remaining parameters were varied through the ranges $0° < |\theta_E| \leq 50°$, $0.5 \leq \ell_o/D_M \leq 1$, and $0 \leq |z_F|/\lambda \leq 5$. Note that, due to the adopted assumptions, the results are symmetric about $z_F = 0$. A linearly-polarized and circularly-symmetric raised-cosine feed model ($\cos^n\theta_F$) was employed as the spherical feed source [7]. Its exponent n was adjusted for every single reflector configuration in order to provide the maximum possible efficiency whenever $z_F = 0$ [4].

The resulting η_A values are shown in Figs. 5–8 for the ADC, ADG, ADE, and ADH, respectively. These figures present contour plots of η_A (values in percent) as a function of $|z_F|/\lambda$, θ_E, and ℓ_o/D_M. For the ADC and the ADE no blockage mechanisms are present (under a GO perspective) [2]. However, for the ADG and, specially, for the ADH the subreflector self blockage is present for smaller values of ℓ_o/D_M, while the feed blockage occurs as $|\theta_E|$ increases [2]. In Figs. 6 and 8, the depicted values of ℓ_o/D_M and $|\theta_E|$ are such that no blockage mechanisms are present whenever $z_F = 0$. From Figs. 5–8 one observes that η_A decreases as $|z_F|/\lambda$ increases, which is expected since the aperture-field distribution becomes more aberrated according to (1). Also, the efficiency decay is less pronounced for smaller values of $|\theta_E|$. This is due to the fact that $|\beta| \to 0$ and $e^2 \to 1$ as $|\theta_E| \to 0$, which agrees with the observation made at the end of Sect. II. Furthermore, the variation of ℓ_o/D_M has a small impact on η_A, as the aperture-field distribution does not vary significantly for $\ell_o/D_M \geq 0.5$ [4].

As GO does not account for diffraction mechanisms, the absolute values of η_A depicted in Figs. 5–8 are expected to be met only in reflector antennas with very large electric dimensions. However, numerical MoM analyses conducted for some representative antenna geometries showed that the relative efficiency decay can be predicted from the previous study with a reasonable accuracy. This is the topic of the next section.

IV. Moment-Method Numerical Analysis of Some Representative Antennas

In order to investigate the accuracy and range of validity of the previous formulation and results, some representative antenna configurations were numerically analyzed by the MoM technique. The analysis was based on the electric field integral equation for bodies of revolution. The raised-cosine feed model used in Sect. III was readopted as the spherical feed source. The antenna geometries were chosen among several analyzed in Sect. III,

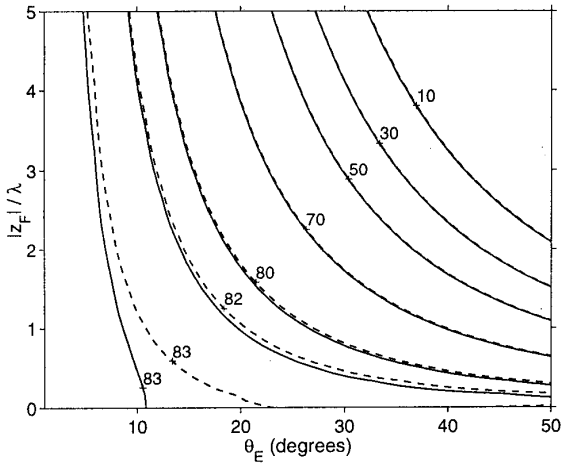

Fig. 5. ADC η_A variation (values in percent) with $|z_F|/\lambda$ and θ_E: $\ell_o/D_M = 0.5$ (solid lines) and 1 (dashed lines).

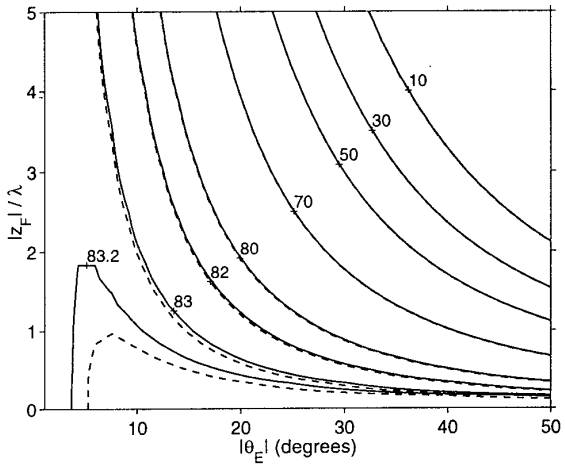

Fig. 6. ADG η_A variation (values in percent) with $|z_F|/\lambda$ and $|\theta_E|$: $\ell_o/D_M = 0.7$ (solid lines) and 1 (dashed lines).

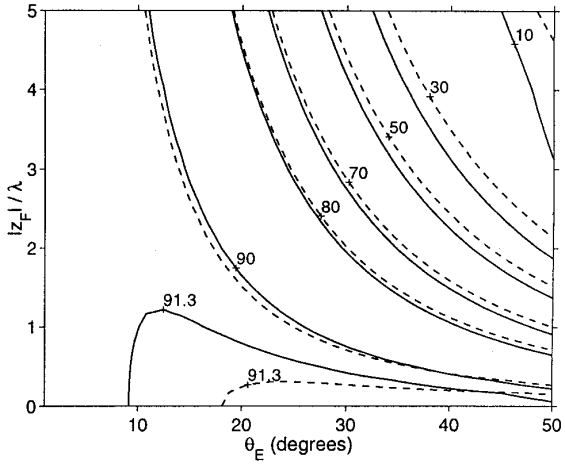

Fig. 7. ADE η_A variation (values in percent) with $|z_F|/\lambda$ and θ_E: $\ell_o/D_M = 0.5$ (solid lines) and 1 (dashed lines).

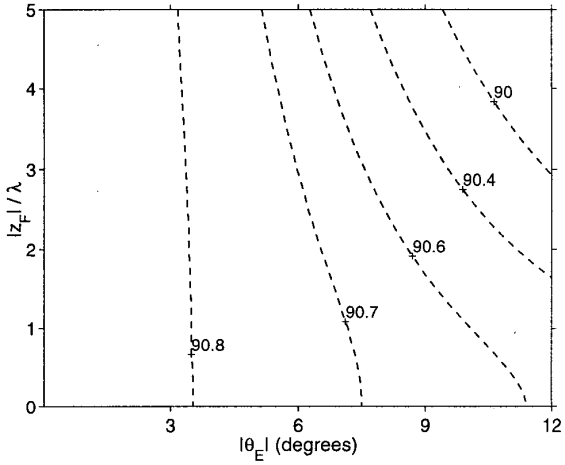

Fig. 8. ADH η_A variation (values in percent) with $|z_F|/\lambda$ and $|\theta_E|$: $\ell_o/D_M = 1$ (dashed lines).

presently with $D_M = 100\lambda$ and $D_B = D_S = 10\lambda$. For all geometries, the main-reflector generating parabola was extended toward the symmetry axis to simulate more realistic configurations. The results for some of the analyzed ADC, ADG, ADE, and ADH antennas (with different pairs ℓ_o, θ_E) are illustrated in Figs. 9–12, respectively. From the figures one observes that the adopted technique reasonably predicts the antenna relative efficiency decay, regarding the MoM results as references. The agreement improves for smaller $|\theta_E|$ angles since the aperture aberration is less pronounced (according to the discussion in Sect. III). For this reason, the reader should not be impressed by the results of Fig. 12, as blockage mechanisms impair ADH configurations with large $|\theta_E|$. Furthermore, the accuracy of the present formulation diminishes as z_F increases, specially when $z_F > 0$. This is basically caused by the change in the aperture amplitude-field distribution, which becomes more accentuated when the feed approaches the subreflector. Another important observation, based on the MoM results, is the general occurrence of maximum efficiencies for feeds slightly defocused toward the subreflector. This is due to the spillover reduction that rapidly occurs before the phase synchronism is lost by defocusing [8].

V. Conclusions

An analytical study of the aperture aberration caused by an axial feed defocusing in generalized classical axially-symmetric dual-reflector antennas was performed. Its consequences to the antenna radiation efficiency were investigated, providing useful results to the antenna design, particularly for issues concerning the feed phase-center displacement. Geometrical conditions were obtained for the reflector surfaces in order to minimize the aperture

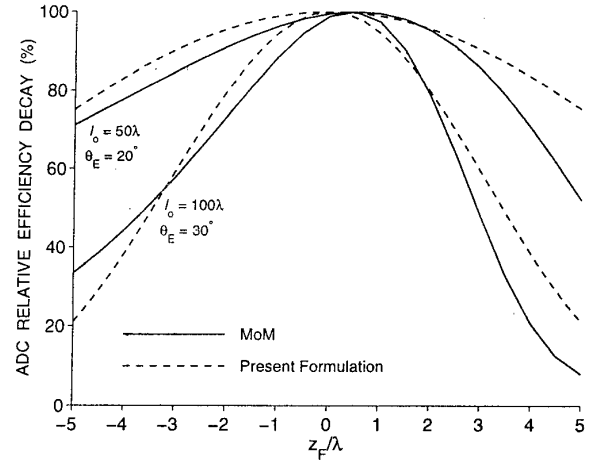

Fig. 9. ADC relative efficiency decay (in percent): MoM (solid lines) and present formulation (dashed lines).

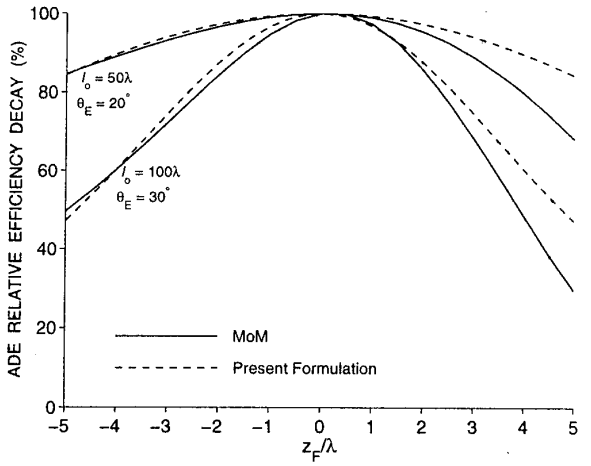

Fig. 11. ADE relative efficiency decay (in percent): MoM (solid lines) and present formulation (dashed lines).

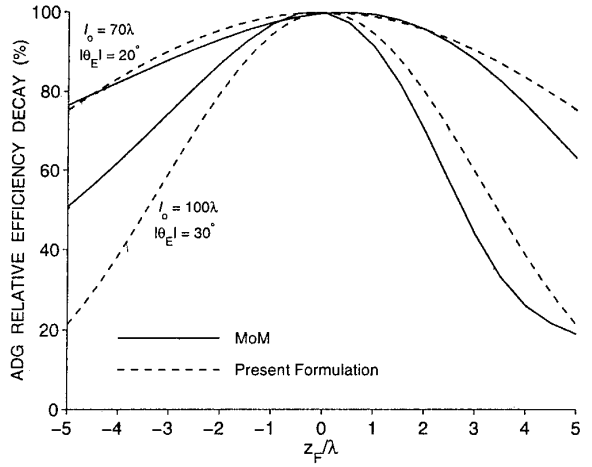

Fig. 10. ADG relative efficiency decay (in percent): MoM (solid lines) and present formulation (dashed lines).

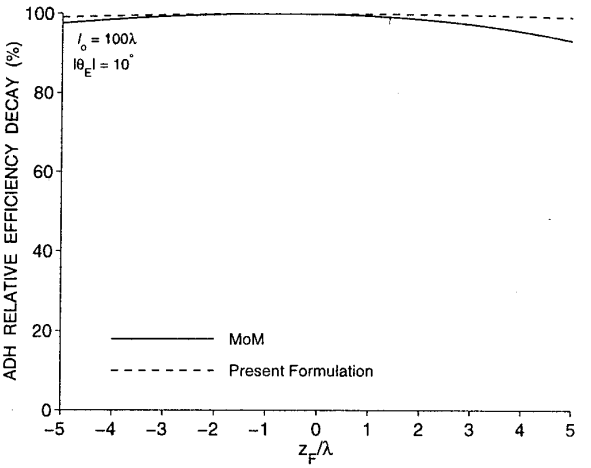

Fig. 12. ADH relative efficiency decay (in percent): MoM (solid lines) and present formulation (dashed lines).

aberration and the associated efficiency decrease. Several representative reflector arrangements were analyzed by the Moment-Method technique to specify the limits of the adopted formulation and to illustrate the general trends of these particular axially-symmetric antennas. It was observed that the relative efficiency decay caused by the feed defocusing can be reasonably predicted, specially for configurations with small subreflector edge-angles. The adopted analysis can be improved (e.g., by considering the aperture amplitude-field variation with the feed axial location). However, simplicity always benefits the acquisition of physical insights necessary for real-case designs.

References

[1] Yu. A. Yerukhimovich, "Analysis of Two-Mirror Antennas of a General Type," Telecommunications and Radio Engineering, Part 2, **27**, No. 11, pp. 97–103, 1972.

[2] F. J. S. Moreira, "Design and Rigorous Analysis of Generalized Axially-Symmetric Dual-Reflector Antennas," Ph.D. dissertation, Univ. Southern California, Los Angeles, Aug. 1997.

[3] F. J. S. Moreira and A. Prata, Jr., "Generalized Classical Axially-Symmetric Dual-Reflector Antennas," 1997 IEEE AP-S Internat. Symp. Digest, Montreal, Canada, pp. 1402–1405, July 1997.

[4] F. J. S. Moreira and A. Prata, Jr., "Maximum-Efficiency Generalized Classical Axially-Symmetric Dual-Reflector Antennas," 10th Internat. Symp. on Antennas (JINA 98), Nice, France, pp. 594–597, Nov. 1998.

[5] C. Dragone, "A First-Order Treatment of Aberrations in Cassegrainian and Gregorian Antennas," IEEE Trans. Antennas Propagat., **AP-30**, No. 3, pp. 331–339, May 1982.

[6] M. Abramowitz and I. A. Stegun (Eds.), *Handbook of Mathematical Functions*, Dover Publications, Inc., New York, eq. 3.6.22.

[7] S. Silver (Ed.), *Microwave Antenna Theory and Design*, Peter Peregrinus, London, 1984, ch. 12.

[8] P. G. Ingerson and W. V. T. Rusch, "Radiation from a Paraboloid with an Axially Defocused Feed," IEEE Trans. Antennas Propagat., **AP-21**, No. 1, pp. 104–106, Jan. 1973.